A Specific Tryptophan in the I-II Linker Is a Key Determinant of β-Subunit Binding and Modulation in $Ca_V2.3$ Calcium Channels

L. Berrou, H. Klein, G. Bernatchez, and L. Parent
Département de Physiologie, Membrane Transport Research Group, Université de Montréal, Montréal, Quebec H3C 3J7, Canada

ABSTRACT The ancillary β subunits modulate the activation and inactivation properties of high-voltage activated (HVA) Ca^{2+} channels in an isoform-specific manner. The β subunits bind to a high-affinity interaction site, α-interaction domain (AID), located in the I-II linker of HVA α1 subunits. Nine residues in the AID motif are absolutely conserved in all HVA channels (QQxExxLxGYxxWIxxxE), but their contribution to β-subunit binding and modulation remains to be established in $Ca_V2.3$. Mutations of W386 to either A, G, Q, R, E, F, or Y in $Ca_V2.3$ disrupted [^{35}S]β3-subunit overlay binding to glutathione S-transferase fusion proteins containing the mutated I-II linker, whereas mutations (single or multiple) of nonconserved residues did not affect the protein-protein interaction with β3. The tryptophan residue at position 386 appears to be an essential determinant as substitutions with hydrophobic (A and G), hydrophilic (Q, R, and E), or aromatic (F and Y) residues yielded the same results. β-Subunit modulation of W386 (A, G, Q, R, E, F, and Y) and Y383 (A and S) mutants was investigated after heterologous expression in *Xenopus* oocytes. All mutant channels expressed large inward Ba^{2+} currents with typical current-voltage properties. Nonetheless, the typical hallmarks of β-subunit modulation, namely the increase in peak currents, the hyperpolarization of peak voltages, and the modulation of the kinetics and voltage dependence of inactivation, were eliminated in all W386 mutants, although they were preserved in part in Y383 (A and S) mutants. Altogether these results suggest that W386 is critical for β-subunit binding and modulation of HVA Ca^{2+} channels.

INTRODUCTION

The influx of calcium through voltage-gated Ca^{2+} channels regulates a wide range of cellular processes, including neurotransmitter release, activation of Ca^{2+}-dependent enzymes and second messenger cascades, gene regulation, and proliferation. To this date, the primary structures for 10 distinct Ca^{2+} channel α_1 subunits have been identified by molecular cloning and were found to fall into three main classes: Ca_V1 with the L-type high-voltage activated Ca^{2+} channels, Ca_V2 with the non-L-type high-voltage activated Ca^{2+} channels, and Ca_V3 with the T-type low-voltage activated Ca^{2+} channels. $Ca_V2.3$ encodes a component of the native R-type current identified in neurons (Randall and Tsien, 1997; Piedras-Renteria and Tsien, 1998; Saegusa et al., 2000) that contributes to the synaptic transmission at hippocampal synapses (Gasparini et al., 2001) and neurohypophysial terminals (Wang et al., 1999). The $Ca_V2.3$ gene is expressed in islets of Langerhans where it could be involved in insulin secretion (Vajna et al., 2001). Knockout mice for $Ca_V3.1$ displayed a decrease in firing at the thalamocortical relay as well as a resistance to absence seizures (Kim et al., 2001).

Although a minimum voltage-gated Ca^{2+} channel can be formed by a single α1 subunit, co-expression of the full complement of subunits is required for the cardiac L-type $Ca_V1.2$ (Biel et al., 1991; Parent et al., 1997), brain N-type $Ca_V2.1$ (Williams et al., 1992; Soong et al., 1993), brain L-type $Ca_V3.1$ (Williams et al., 1992; Bell et al., 2001; Beguin et al., 2001), and R-type $Ca_V2.3$ (Parent et al., 1997) to generate Ca^{2+} currents with time course and voltage dependence similar to native currents (Catterall, 1991). β-Subunits increase current density (Brice et al., 1997; Tareilus et al., 1997; Bichet et al., 2000a) by antagonizing an endoplasmic reticulum retention signal that is contained within the I-II linker (Bichet et al., 2000a). β-Subunits hyperpolarize the voltage dependence of activation and inactivation, except for β2a, which decreases the kinetics and the voltage dependence of inactivation in $Ca_V2.1$–2.3 (Parent et al., 1997; Mangoni et al., 1997; DeWaard and Campbell, 1995; Stea et al., 1994; Jones et al., 1998; Cens et al., 1999). The mechanism underlying this effect is probably related to the palmytoylation of the cysteines 3 and 4 in the N-terminal of β2a (Chien et al., 1996; Restituito et al., 2000; Qin et al., 1998; Chien and Hosey, 1998; Stephens et al., 2000).

The auxiliary β subunits can potentially be associated with any of the six α1 pore-forming subunits of high-voltage Ca^{2+} channels ($Ca_V1.1$- 1.3; $Ca_V2.1$- 2.3) via conserved interaction domains: α-interaction domain (AID) located on the I-II linker of the α1 subunit and the β-interaction domain (BID) located at the beginning of the second conserved region of the β subunit (DeWaard et al., 1995, 1996; Pragnell et al., 1994; Walker and DeWaard, 1998; Walker et al., 1998, 1999). The AID binding site is composed of QQxExxLxGYxxWIxxxE where x can be any residue (see Fig. 1 *A*). Point mutations of conserved (Q374, Q375, E377, L380, G382, E391) or nonconserved (R378) residues within the AID motif failed to alter the binding of

Submitted April 6, 2002, and accepted for publication May 21, 2002.

H.K. and G.B. contributed equally to this work.

Address reprint requests to Dr. L. Parent, Département de Physiologie, Membrane Transport Research Group, Université de Montréal, P.O. Box 6128, Downtown Station, Montréal, Qué. H3C 3J7, Canada. Tel.: 514-343-6673; Fax: 514-343-7146; E-mail: lucie.parent@umontreal.ca.

0006-3495/02/09/1429/14 $2.00

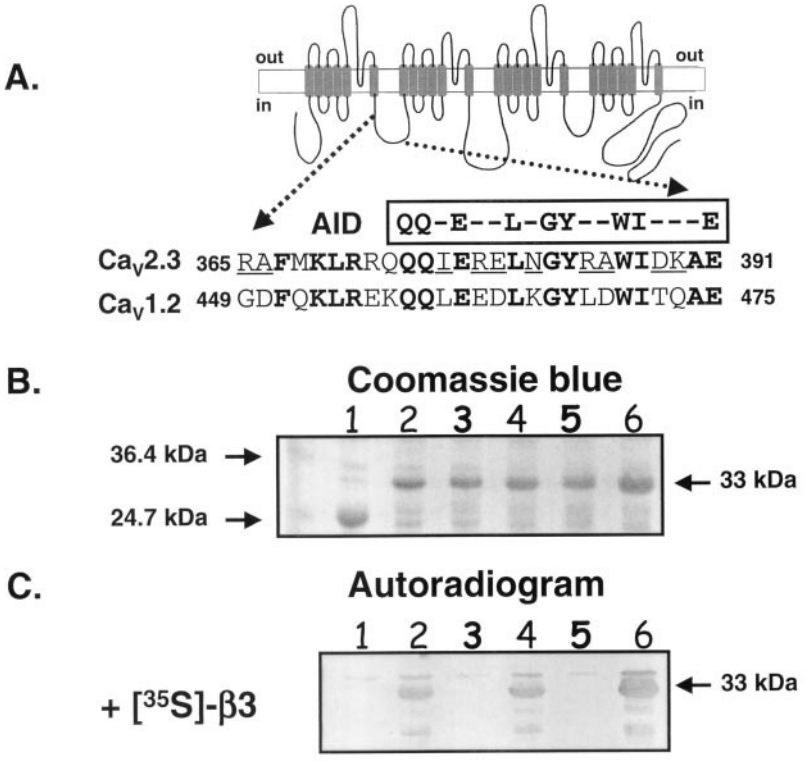

FIGURE 1 β3-Subunit binding to the I-II linker of $Ca_V2.3$. (*A*) Predicted secondary structure for the human brain $Ca_V2.3$ channel with the four homologous repeats and the N- and the C-termini facing the cytoplasm. The β-subunit binding site on the α1 subunit (AID) is located within 20 residues of the IS6 transmembrane segment. The consensus sequence for the AID motif (QQxExxLxGYxxWIxxxE) is shown for $Ca_V2.3$ and $Ca_V1.2$ with conserved residues in bold letters. The residues mutated in the decatuple mutant RAIRENRADK-GDLEDKLDTQ (365–389) are underlined. (*B*) Coomassie blue-stained SDS-PAGE gel showing the wild-type and the mutant AID fusion proteins from $Ca_V2.3$. Molecular weight standards are shown to the left. The GST-proteins have a molecular mass of 25 kDa (no insert) or 33 kDa (87 AA from the I-II linker). (*C*) Autoradiogram of in vitro translated [^{35}S]β3 overlays on AID_E GST-I-II mutants immobilized on nitrocellulose. Whereas a strong signal was recorded for the wild-type channel, R378E, and RAIRENRADK-GDLEDKLDTQ, [^{35}S]β3 binding could not be detected for W386A. *Lane 1*, pGEX-4T1 vector; *lane 2*, wild-type $Ca_V2.3$; *lane 3*, W386A; *lane 4*, R378E; *lane 5*, W386A; *lane 6*, the decatuple mutant RAIRENRADK-GDLEDKLDTQ.

β3 to $Ca_V2.1$ (Bichet et al., 2000a). In contrast, the YWI residues appear to be critical for β1b and/or β3 binding in $Ca_V2.1$ (DeWaard et al., 1996). Mutations of the conserved tyrosine (Y383) residue to a serine (S) disrupted β3 binding to $Ca_V2.1$, although the substitution by a phenylalanine (F) or a tryptophan (W) preserved in part β3 and β1b binding (DeWaard et al., 1996; Witcher et al., 1995). The Y to S substitution in the AID motif of $Ca_V1.2$ and $Ca_V1.1$ disrupted the plasma membrane localization of the α1 subunit while preserving in part the β-subunit-induced modulation of whole-cell and single-channel currents (Neuhuber et al., 1998a,b; Gerster et al., 1999).

Mutations and deletions within the AID motif (see Fig. 1 *A*) were shown to disrupt the voltage dependence of inactivation in high-voltage activated (HVA) Ca^{2+} channels (Page et al., 1997; Geib et al., 2002; Berrou et al., 2001; Herlitze et al., 1997). We have recently shown that mutations of the nonconserved R378 in the AID motif specifically decreased the kinetics and voltage dependence of inactivation in $Ca_V2.3$, whereas the E462R mutation in $Ca_V1.2$ accelerated inactivation kinetics (Berrou et al., 2001; Bernatchez et al., 2001b). Despite being enclosed within the AID motif, $Ca_V2.3$ R378E, $Ca_V1.2$ E462R, and $Ca_V1.2/Ca_V2.3$ chimeras were found to be typically modulated by β subunits in terms of the kinetics and the voltage dependence of inactivation (Berrou et al., 2001; Bernatchez et al., 2001a). Although the β-subunit binding properties of the AID locus have been well established in $Ca_V2.1$, its role in regard to β-subunit binding and modulation remains to be investigated in $Ca_V2.3$.

We show here that point mutations of W386 disrupted β-subunit binding to the I-II linker. Furthermore, the tryptophan residue appears to be an essential determinant at position 386 as substitutions with hydrophobic (A, G), hydrophilic (Q, R,E), and aromatic (F, Y) residues alike led to the same results. In contrast, the nonconserved mutations R378E and the multiple mutant R365G + A366D + I376L + R378E + E379D + N381K + R384L + A385D + D388T + K389Q preserved β-subunit binding (see Fig. 1). When expressed in *Xenopus* oocytes, W386 mutants (A, G,

Q, R, E, F, Y) and Y383 (A, S) yielded large whole-cell Ba^{2+} currents with typical current-voltage properties. β3-Subunit modulation of inactivation was eliminated in W386 mutants but not in Y383 mutants, suggesting that W386 is critical for β-subunit binding and modulation of $Ca_V2.3$ channels.

MATERIALS AND METHODS

Recombinant DNA materials

Standard methods of plasmid DNA preparation were used (Sambrook et al., 1989). cDNAs coding for the auxiliary β3 (Genbank M88751) and β2a (Genbank M80545) were kindly donated by Dr. E. Perez-Reyes (Castellano et al., 1993; Perez-Reyes et al., 1992). The wild-type human $Ca_V2.3$ (α1E) (GenBank L27745) was a gift from Dr. T. Schneider (Schneider et al., 1994). The rat brain α2bδ subunit was provided by Dr. T. P. Snutch.

Point mutations and RNA transcription

Point mutations were performed with 35–40-mer synthetic oligos into the wild-type $Ca_V2.3$ using the Quick-Change XL-mutagenesis kit (Stratagene, La Jolla, CA). The nucleotide sequence of the mutant channel was bi-directionally analyzed using automatic sequencing by BioST (Lachine, Québec, Canada). cDNA constructs for wild-type and mutated α1 subunits were linearized at the 3′ end by *Hin*dIII digestion whereas the β3 and β2a subunits were digested by *Not*I. Run-off transcripts were prepared using methylated cap analog $m^7G(5')ppp(5')G$ and T7 RNA polymerase with the mMessage mMachine transcription kit (Ambion, Austin, TX). The final cRNA products were resuspended in DEPC-treated H_2O and stored at −80°C. The integrity of the final product and the absence of degraded RNA were determined by a denaturing agarose gel stained with ethidium bromide.

β3 overlay assays onto glutathione S-transferase (GST) fusion proteins

A fragment encoding the amino acids 338–425 in $Ca_V2.3$ was generated by polymerase chain reaction, cloned in-frame into the *Bam*HI-*Xho*I sites of pGEX-4T1 vector (Amersham Pharmacia Biotech, Baie-D'urfée, Québec, Canada) and expressed in the *Escherichia coli* strain BL21-De3. The synthesis of the fusion proteins was induced using 0.5 mM isopropyl β-D-thiogalactoside in a liquid culture grown to A_{600} of ~1.0. After 2.5 h at 37°C, bacteria were collected by centrifugation. For overlay assays, crude BL21 bacterial extracts were boiled for 2 min in 2X Laemmli's loading buffer and separated on a denaturing SDS-polyacrylamide gel (12% acrylamide). Samples were loaded in duplicate so the proteins could be visualized by Coomassie staining in addition to the autoradiogram. This half of the gel was transferred onto a PVDF membrane (Millipore GmbH, Eschborn, Germany) using Towbin buffer (25 mM Tris, 192 mM glycine, 20% methanol, and 0.05% SDS). The membrane was blocked with 1% bovine serum albumin (BSA) in HBS-Tween (137 mM NaCl, 3 mM KCl, 10 mM HEPES, and 0.05% Tween-20, pH 7.4), washed once with HBS-Tween and incubated for 1 h at room temperature in 5 ml of HBS-Tween with 20 μl of [^{35}S]methionine-labeled β3 subunit. The blots were washed twice for 10 min in HBS-Tween and air dried, and radioactive signals were detected by autoradiography. ^{35}[S]Methionine-labeled β3 in pBluescript (0.5 μg) was synthesized by coupled in vitro transcription and translation (TNT Promega, Madison, WI) in a 50-μl reaction volume for 1 h, and the reaction mixture was applied without further treatment to the overlay membrane. To ensure equivalent protein loading, gels were stained with Coomassie blue to visualize the major protein band in each lane before autoradiography.

Functional expression of wild-type and mutant channels

Oocytes were obtained from female *Xenopus laevis* clawed frog (Nasco, Fort Atkinson, WI) as described previously (Parent et al., 1995, 1997; Berrou et al., 2001; Bernatchez et al., 1998, 2001a; Jean et al., 2002). Briefly, stage VI oocytes free of follicular cells were injected with 46 nl of a solution containing between 35 and 50 ng of cRNA coding for the wild-type or mutated α1 subunit. The α1 subunit was always co-injected with cRNA coding for the rat brain α2bδ (Williams et al., 1992) and either with the rat brain β3 (Castellano et al., 1993) or the rat β2a (Perez-Reyes et al., 1992) in a 3:1:1 weight ratio, respectively. Oocytes were incubated at 19°C in a Barth's solution: 100 mM NaCl, 2 mM KCl, 1.8 mM $CaCl_2$, 1 mM $MgCl_2$, 5 mM HEPES, 2.5 mM pyruvic acid, 100 U/ml penicillin, 50 μg/ml gentamicin, pH 7.6.

Electrophysiological recordings in oocytes

Wild-type and mutant channels were screened at room temperature for macroscopic barium current 4–7 days after RNA injection using a two-electrode voltage-clamp amplifier (OC-725C, Warner Instruments, Hamden, CT) as described earlier (Parent et al., 1995, 1997; Berrou et al., 2001; Jean et al., 2002). Oocytes were first impaled in a modified Ringer solution (in mM: 96 NaOH, 2 KOH 1.8 $CaCl_2$, 1 $MgCl_2$, 10 HEPES) titrated to pH 7.4 with methanesulfonic acid CH_3SO_3H (MeS). The bath was then perfused with the 10 mM Ba^{2+} solution (in mM: 10 $Ba(OH)_2$, 110 NaOH, 1 KOH, 20 HEPES) titrated to pH 7.3 with MeS. To minimize kinetic contamination by the endogenous Ca^{2+}-activated Cl^- current, oocytes were injected with 18.4 nl of a 50 mM EGTA (Sigma, St. Louis, MO) 0.5–2 h before the experiments. Oocytes were superfused by gravity flow at a rate of 2 ml/min, which was fast enough to allow complete chamber fluid exchange within 30 s. Experiments were performed at room temperature (20–22°C).

Data acquisition and analysis

PClamp software, Clampex 6.02 and Clampfit 6.02 (Axon Instruments, Foster City, CA) was used for online data acquisition and analysis as previously described (Bernatchez et al., 2001a,b; Berrou et al., 2001; Jean et al., 2002). Unless stated otherwise, data were sampled at 10 kHz and low pass filtered at 5 kHz using the amplifier built-in filter. For all recordings, a series of voltage pulses were applied from a holding potential of −80 mV at a frequency of 0.2 Hz from −40 to +60 mV. Isochronal inactivation data (h_∞ or h inf) were obtained from tail currents generated at the end of a 5-s prepulse (Parent et al., 1995, 1997). Tail current amplitudes were estimated using the function Analyze in Clampfit 6.0 from the peak current arising during the first 10 ms after the capacitive transient (20 data points). Each of these currents was then normalized to the maximum current obtained before the prepulse voltage (i/i_{max}) and was plotted against the prepulse voltage. For the isochronal inactivation figures, data points represent the mean of $n \geq 3$ and were fitted to the Boltzmann Eq. 1:

$$\frac{I}{I_{max}} = 1 - \frac{(1 - Y_o)}{1 + e^{\frac{-zF(V_m - E_{0.5,inact})}{RT}}}. \quad (1)$$

Pooled data points (mean ± SEM) were fitted to Eq. 1 using user-defined functions and the fitting algorithms provided by Origin 6.0 (Microcal Software) analysis software. Equation 1 accounts for the fraction of non-inactivating current with $E_{0.5,inact}$ mid-point potential; z, slope parameter; Y_0, fraction of non-inactivating current; V_m, the prepulse potential; and

RT/F with their usual meanings. The fitting process generated values estimating errors on the given fit values.

Activation potentials were estimated from the normalized *I-V* curves obtained for each channel combination (Canti et al., 2001). Although this calculation was not exempt from gating contamination, it provided a qualitative approximation of the β3 modulation on *I-V* parameters. The *I-V* relationships were normalized to the maximum amplitude and were fitted to Eq. 2, a Boltzmann equation coupled to a linear function:

$$\frac{I}{I_{max}} = G_{rel}\frac{(V_m - V_{rev})}{1 + e^{\frac{-zF(V_m - E_{0.5,act})}{RT}}}, \quad (2)$$

where $E_{0.5,act}$ is the potential for 50% activation, G_{rel} is the normalized conductance, z is slope parameter, V_m is the test potential, V_{rev} is the apparent reversal potential, and RT/F have their usual meanings.

Inactivation kinetics were quantified using r300 values, that is the ratio of the whole-cell current remaining at the end of a 300-ms pulse (Berrou et al., 2001; Bernatchez et al., 2001a,b). As inactivation kinetics can vary with current density, comparisons between constructs and mutants were generally restricted to whole-cell currents lower than 5 μA as much as possible. Furthermore, this range of current densities made it easier to voltage clamp the oocyte uniformly, thus decreasing the possibility of series resistance artifacts contaminating the current kinetics data. Capacitive transients were erased for clarity in the final figures. Statistical analyses and Student *t*-test were performed using the fitting routines provided by Origin 6.1 (Microcal Software, Northampton, MA).

RESULTS

β-Subunit overlay assays in the I-II linker of $Ca_V2.3$

We have recently shown that the nonconserved residue R378 within the AID motif of $Ca_V2.3$ channels disrupted specifically the kinetics and voltage dependence of inactivation, whereas the reverse mutation E462R in $Ca_V1.2$ accelerated inactivation kinetics (Berrou et al., 2001; Bernatchez et al., 2001a). Among nonconserved residues of the AID motif, R378 in $Ca_V2.3$ was shown to be particularly critical as multiple mutations of other nonconserved residues failed to significantly affect the kinetics and voltage dependence of inactivation (Berrou et al., 2001). To evaluate whether such mutations could have altered β-subunit binding to the I-II linker, we constructed one series of GST fusion proteins containing 87 amino acids (AA) (338–428 in AA) between IS6 and the middle of the I-II linker of $Ca_V2.3$ (GST-AID_E). Because the GST fusion proteins are denatured before being transferred onto a nitrocellulose blot, overlay assays suggest that β3 binding to the I-II linker does not depend too critically upon the secondary structure of the AID motif. As seen in Fig. 1, in vitro translated ^{35}[S]methionine β3 could bind to the wild-type GST-AID_E, the GST-AID(R378E), and the multiple mutant GST-AID_C (R365G + A366D + I376L + R378E + E379D + N381K + R384L + A385D + D388T + K389Q) (RAIRENRADK-GDLEDKLDTQ), which includes all the nonconserved residues within the AID motif mutated to their counterparts in $Ca_V1.2$. In contrast, there was no discernible binding of radiolabeled β3 to the GST-AID(W386A). Hence our results with $Ca_V2.3$ generally agree with data previously reported for $Ca_V2.1$ where β-subunit binding to the I-II linker was found to depend upon the conserved WYI residues and not to be critically dependent upon the nature of the intervening sequences within the AID motif (DeWaard et al., 1995).

W386A mutation impairs β-subunit binding and modulation of $Ca_V2.3$

Correlation between β-subunit binding and modulation was investigated in the following series of experiments. As shown in Fig. 2, the W386A $Ca_V2.3$ channel was expressed with or without (±) β3 or β2a in *Xenopus* oocytes. Whole-cell current traces of the wild-type $Ca_V2.3$ and the R378E mutant are shown alongside for comparison. Expression of the W386A mutant yielded robust inward Ba^{2+} currents with current-voltage relationships typical of voltage-gated Ca^{2+} channels. In the absence of exogenous β subunits, the W386A, R378E, and wild-type $Ca_V2.3$ channels activated within the same voltage range. The complete set of activation potentials is shown in Table 1. W386A/α2bδ activated at $E_{0.5} = -7 \pm 1$ mV ($n = 7$), which is similar to $E_{0.5} = -6 \pm 2$ mV ($n = 10$) for $Ca_V2.3$wt/α2bδ currents (see also Parent et al., 1997; Berrou et al., 2001). Hence in the absence of exogenous β3, the activation parameters of W386A, R378E, and wild-type $Ca_V2.3$ channels were comparable. In contrast, β3 induced a significant hyperpolarizing shift in the $E_{0.5,act}$ values of R378E and $Ca_V2.3$ wild type, whereas it did not affect W386A. Furthermore, coexpression with β3 failed to significantly increase Ba^{2+} peak currents of W386A (Table 1).

In $Ca_V2.3$ channels, β−subunit modulation of inactivation, kinetics, and voltage dependence is isoform specific with β3 accelerating inactivation and β2a slowing it down (Olcese et al., 1994; Parent et al., 1997). In this regard, R378E behaved like $Ca_V2.3$wt with r300 values smaller in the presence of β3 and significantly larger with β2a (Fig. 3). Furthermore, the R378E channel displayed slower inactivation kinetics than $Ca_V2.3$wt under the same subunit background, in agreement with our previous study (Berrou et al., 2001). In contrast, the inactivation kinetics of W386A were not significantly affected by β3 or β2a subunit or significantly modulated by the membrane potential. Although its inactivation kinetics was slower than $Ca_V2.3$/α2bδ, W386A/α2bδ displayed significantly faster inactivation than R378E/α2bδ, thus confirming the key role of R378 in the voltage-dependent inactivation of $Ca_V2.3$. As shown in greater detail later, this conclusion is supported by the functional characterization of the seven mutants made at position W386 as well as for the two Y383 mutants.

Finally, the voltage dependence of inactivation was measured for W386A, R378E, and the wild-type channel in the presence and in the absence of β3 using 5-s prepulses. The midpoints of inactivation ($E_{0.5,inact}$) estimated from the

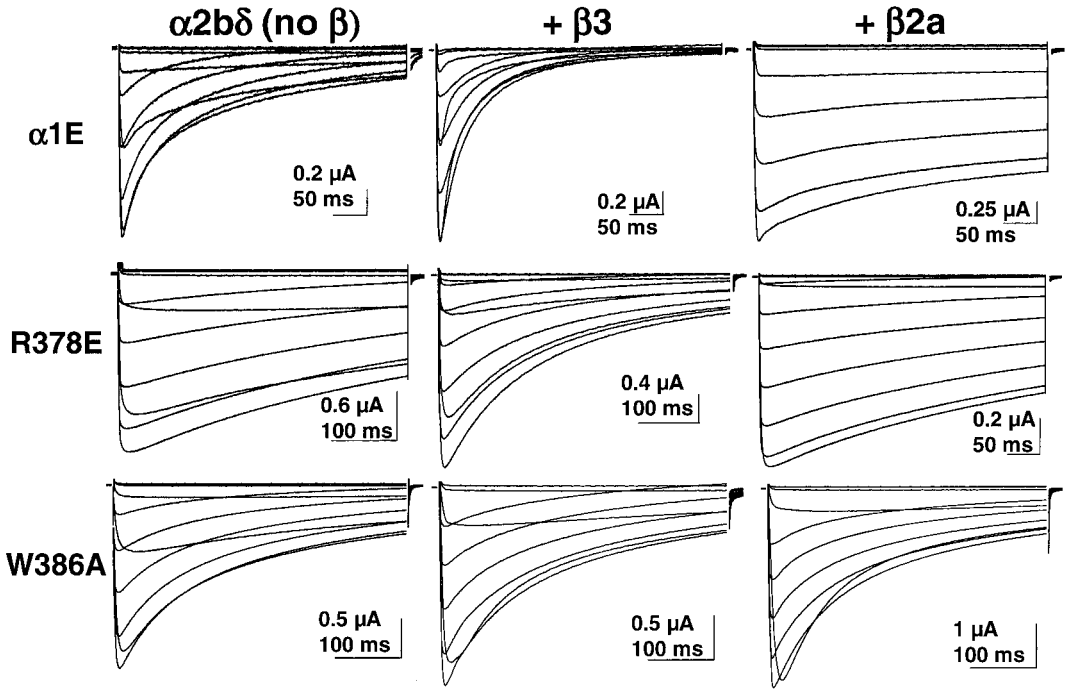

FIGURE 2 Lack of β-subunit-induced modulation in W386A channels. The wild-type $Ca_V2.3$ (*first row*), R378E (*second row*), and W386A (*third row*) were expressed in *Xenopus* oocytes in the presence of α2bδ without β subunits (*left panel*), α2bδ + β3 (*middle panel*), or α2bδ + β2a (*right panel*). The average peak current densities are given in Table 1. In the absence of β subunits, the r300 ratios ranked R378E > W386A > wild type (from the slowest to the fastest). The inactivation kinetics of W386A remained insensitive to the presence of either β3 or β2a. In contrast, the inactivation kinetics of R378E were accelerated by β3 and slowed by β2a in a manner similar to the wild-type channel. Whole-cell currents were recorded using the two-electrode voltage-clamp technique in the presence of 10 mM Ba^{2+} after injection of EGTA. Holding potential was −80 mV. Oocytes were pulsed from −40 mV to +60 mV using 10-mV steps for 450 ms. All mutants expressed significant inward currents with typical current-voltage properties. Capacitive transients were erased for the first millisecond after the voltage step.

pooled data are shown in Table 1. As seen, coexpression with β3 did not shift the inactivation curves for W386A with $E_{0.5,inact} = -39 \pm 2$ mV ($n = 6$) for W386A/α2bδ as compared with $E_{0.5,inact} = -35 \pm 1$ mV ($n = 6$) for W386A/α2bδ/β3 channels. In contrast, the $E_{0.5,inact}$ values for R378E and the wild-type channels were shifted to the left by 20–30 mV in the presence of β3. Hence mutation of W386 in the AID motif was found to significantly decrease if not eliminate β-subunit binding and modulation in $Ca_V2.3$ channels.

Functional properties of the double R378E + W386A mutant

To investigate the relationships between β-subunit modulation and the inactivation properties conferred by the I-II linker, the double mutant R378E + W386A was expressed and functionally characterized in *Xenopus* oocytes with or without exogenous β3 (Fig. 4, *A* and *B*). The double mutant retained the dominant features of both channels, namely, the slower inactivation kinetics of R378E coupled to the absence of β-subunit-induced modulation of W386A (Fig. 4 *C* and Table 1). As seen, the activation and inactivation properties of R378E + W386A were not modulated by β3 as was seen for W386A. The voltage dependence of inactivation of R378E + W386A/α2bδ ± β3 was similar to R378E/α2bδ but significantly less negative than W386A ±β3 or $Ca_V2.3$ wt/α2bδ as it was shifted to the right by ~+20 mV (Berrou et al., 2001). Hence, mutating two neighboring sites in the I-II linker did not alter further the inactivation properties of $Ca_V2.3$, suggesting that inactivation and β-subunit modulation are controlled by distinct loci on the α1 subunit of $Ca_V2.3$.

β3-Subunit modulation of inactivation in Y383 mutants

Mutations of the conserved tyrosine (Y) were shown to preserve in part β-subunit binding (Witcher et al., 1995) to AID_A- and β-subunit-induced modulation of the voltage dependence of inactivation in L-type $Ca_V1.1$ and $Ca_V1.2$ (Neuhuber et al., 1998a). β-Subunit modulation was characterized after functional expression of the mutants in *Xenopus* oocytes. Whole-cell current traces for Y383S ± β3 (not shown) and Y383A ± β3 channels were typical of HVA Ca^{2+} channels. β3 subunits did not

TABLE 1 Biophysical parameters of $Ca_V2.3$ wild-type and mutant channels expressed in *Xenopus oocytes* in the presence of $\alpha 2b\delta$ and ± $\beta 3$ subunits

Coexpressed with $\alpha 2b\delta$ (10 Ba^{2+})	Inactivation (5s) $E_{0.5}$ (mV)		Activation $E_{0.5}$ (mV)		Peak I_{Ba} (μA)		Binding $[^{35}S]\beta 3$
	$-\beta 3$	$+\beta 3$	$-\beta 3$	$+\beta 3$	$-\beta 3$	$+\beta 3$	
$\alpha 1E$ wt	−36 ± 3	−64 ± 2	−6 ± 2	−16 ± 2	−1.5 ± 0.3	−3.6 ± 0.5	++
	(10)	(10)	(10)	(10)	(10)	(10)	
	$z = 2.8$	$z = 3.1$	$z = 4.1$	$z = 5.6$			
$\alpha 1E$ R378E	−26 ± 2	−44 ± 2	−3 ± 1	−11 ± 2	−2.9 ± 0.5	−4.7 ± 0.6	++
	(7)	(11)	(5)	(11)	(7)	(11)	
	$z = 2.9$	$z = 2.8$	$z = 4.1$	$z = 5.1$			
$\alpha 1E$ W386A	−39 ± 2	−35 ± 1	−7 ± 1	−7 ± 1	−1.6 ± 0.9	−2.1 ± 0.8	No
	(7)	(6)	(7)	(7)	(7)	(6)	
	$z = 2.7$	$z = 2.5$	$z = 4.4$	$z = 4.2$			
$\alpha 1E$ W386G	−27 ± 1	−29 ± 1	−1 ± 1	−3 ± 1	−1.5 ± 0.2	−1.2 ± 0.3	No
	(4)	(5)	(4)	(4)	(4)	(4)	
	$z = 2.9$	$z = 3.1$	$z = 4.2$	$z = 4.5$			
$\alpha 1E$ W386Q	−31 ± 1	−31 ± 1	0 ± 1	−1 ± 1	−1.2 ± 0.3	−1.5 ± 0.3	No
	(3)	(4)	(5)	(4)	(5)	(4)	
	$z = 2.6$	$z = 2.7$	$z = 3.8$	$z = 3.9$			
$\alpha 1E$ W386E	−27 ± 1	−28 ± 1	−3 ± 2	−5 ± 2	−6 ± 3	−4 ± 2	No
	(6)	(6)	(7)	(7)	(5)	(5)	
	$z = 2.8$	$z = 2.7$	$z = 5.2$	$z = 4.5$			
$\alpha 1E$ W386R	−37 ± 1	−37 ± 1	−7 ± 3	1 ± 2	−1.4 ± 0.2	−1.4 ± 0.3	No
	(3)	(3)	(4)	(4)	(7)	(6)	
	$z = 2.7$	$z = 2.5$	$z = 3.7$	$z = 3.8$			
$\alpha 1E$ W386F	−36 ± 1	−37 ± 1	−1 ± 2	−4 ± 1	−1.1 ± 0.2	−1.9 ± 0.2*	No
	(6)	(3)	(4)	(5)	(5)	(7)	
	$z = 2.6$	$z = 2.7$	$z = 3.9$	$z = 4.3$			
$\alpha 1E$ W386Y	−45 ± 1	−46 ± 1	−2 ± 1	−2 ± 1	−3.2 ± 0.4	−2.5 ± 0.7	No
	(7)	(7)	(8)	(7)	(7)	(7)	
	$z = 2.7$	$z = 2.4$	$z = 4.3$	$z = 4.3$			
$\alpha 1E$ Y383A	−55 ± 1	−32 ± 1	−4 ± 1	−5 ± 1	−1.1 ± 0.2	−1.0 ± 0.1	No
	(4)	(4)	(4)	(4)	(4)	(4)	
	$z = 2.1$	$z = 2.2$	$z = 3.8$	$z = 4.2$			
$\alpha 1E$ Y383S	−42 ± 2	−24 ± 1	−4 ± 1	−7 ± 3	−3 ± 2	−1.6 ± 0.4	No
	(4)	(4)	(4)	(4)	(4)	(4)	
	$z = 1.8$	$z = 2.5$	$z = 4.9$	$z = 4.1$			
R378E + W386A	−22 ± 2	−23 ± 1	−4 ± 2	0 ± 1	−3.0 ± 0.9	−1.8 ± 0.9	No
	(4)	(4)	(4)	(4)	(4)	(4)	
	$z = 2.4$	$z = 2.4$	$z = 4.1$	$z = 3.9$			

Whole-cell currents were measured in 10 mM Ba^{2+} throughout. The voltage-dependence of inactivation was determined by fitting the relative tail currents (5-s pulses) to the Boltzmann equation (Eq. 1). The activation parameters were determined using the modified Boltzmann equation (Eq. 2). The reversion potentials (V_{rev}) estimated from this fit ranged from 45 to 55 mV.

*Peak I_{Ba} was determined from *I–V* relationships for the corresponding experiments usually within 12 hr except for W386F + $\beta 3$, where peak current expression was delayed by 24 hr as compared to W386F no $\beta 3$. The data are shown with the mean ± SEM and the number of samples, *n*, appears in parentheses.

significantly hyperpolarize the activation potentials of either Y383A or Y383S channels (Table 1). However, $\beta 3$ appeared to modulate the inactivation kinetics of Y383A, although it did not influence Y383S as shown on the r300 graph (Fig. 5 *C*). Furthermore, coexpression with $\beta 3$ induced a significant hyperpolarizing shift of −20 mV in the voltage dependence of inactivation for both Y383A and Y383S channels (Fig. 5 *D*), indicating that functional modulation by $\beta 3$ was preserved in part in Y383 mutants. The results obtained with $Ca_V2.3$ differ somehow with $Ca_V1.2$ (Gerster et al., 1999). In that last study, the inactivation kinetics of the Y467S mutant in $Ca_V1.2$ was reported to be typically modulated by β subunits, whereas the voltage dependence of inactivation remained insensitive to β subunits (Gerster et al., 1999). Nonetheless, it can be concluded that mutating the conserved Y residue does not eliminate β-subunit modulation in HVA Ca^{2+} channels.

Molecular determinants of β-subunit binding and modulation in W386 mutants

The alanine mutation at position W386 was shown to disrupt $\beta 3$-subunit binding as well as $\beta 3$- and $\beta 2a$-subunit-induced modulation of $Ca_V2.3$. The structural re-

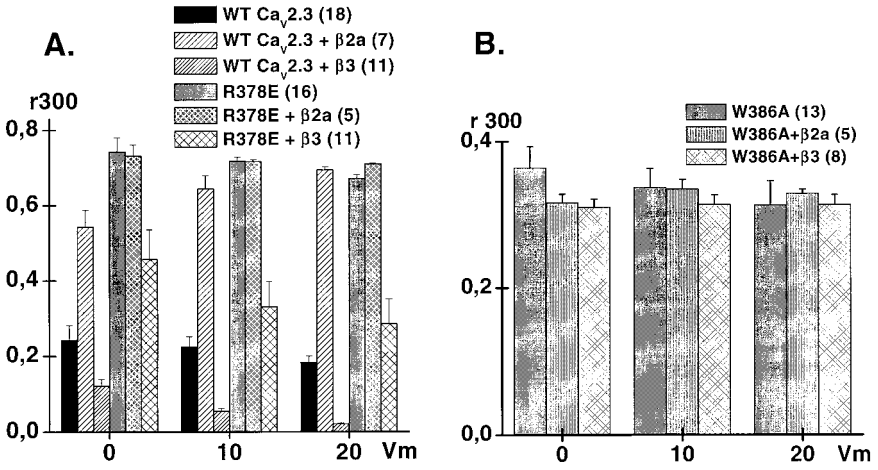

FIGURE 3 Inactivation kinetics of W386A were not modulated by β3 or β2a. (*A*) The mean r300 ratios (the fraction of the whole-cell current remaining at the end of a 300-ms pulse) are shown ± SEM from 0 to +20 mV for $Ca_V2.3$ wt (black) and $Ca_V2.3$ R378E (gray) in the absence and in the presence of β2a or β3. Co-injection with either β2a or β3 led to significant changes ($p < 0.001$) in the r300 values for the wild-type channels at all voltages. β3 sped up inactivation kinetics of R378E ($p < 0.001$), but β2a had no significant effect. (*B*) The mean r300 ratios failed to show any significant modulation of inactivation of W386A channels by β3 or β2a at +10 or +20 mV. The apparent decrease in r300 values at 0 mV was significant only at $p < 0.05$. No significant acceleration of inactivation kinetics was observed with increased depolarization under any condition. Whole-cell currents were measured in 10 mM Ba^{2+}. The numbers to the left of the mutants refer to the numbers of experiments used for statistical analysis.

quirements for β-subunit binding and modulation were next investigated at position W386 after substitutions with hydrophobic (A, G), hydrophilic (Q, R, E), and aromatic (F, Y) residues. [^{35}S]β3 binding to GST fusion proteins mutated to W386A, W386E, W386G, W386F, W386Y, or W386Q is shown in Fig. 6. Coomassie blue stained SDS-PAGE gel attests that the GST-mutants were all expressed as 33-kDa proteins and that gel loading was equivalent in each lane. None of the mutants displayed any discernible trace of β3 overlay binding although [^{35}S]β3 binding on the control wild-type channel was observed under the same experimental conditions.

W386 mutants were expressed ±β3 and characterized in *Xenopus* oocytes (Fig. 7). All W386 mutants, including W386R and W386F (not shown), expressed robust inward currents in the presence of 10 mM Ba^{2+}. In this regard, peak current expression was found to vary widely from day to day as compared with the wild-type channel recorded under the same conditions. The mean current-voltage relationships of the W386 mutants were not significantly shifted in the hyperpolarized direction by β3. As seen for W386A, the activation potentials for the W386 mutants were generally in the same range as the $Ca_V2.3/\alpha2b\delta$ channels without any significant modulation by β3 with the exception of W386R, which showed a reverse sensitivity to β3 (Table 1).

The kinetics (Fig. 8 *A*) and voltage dependence of inactivation (Fig. 8 *B*) of W386 mutants were also poorly modulated by β3. As seen at 0 mV, inactivation kinetics was similar for W386A ± β3, W386E ± β3, W386G ± β3, and W386Y ± β3 with ~30% of the whole-cell currents remaining at the end of a 300-ms pulse. β3 did not increase their inactivation kinetics ($p > 0.1$) in contrast to the fourfold acceleration experienced by the wild-type channel ($p < 10^{-4}$). Some W386 mutants behaved distinctively. For instance, the inactivation kinetics of W386A ± β3 and W386E ± β3 were distinctively voltage independent, whereas W386G ± β3 and W386Y ± β3 appeared to inactivate significantly faster with depolarization ($p < 10^{-3}$).

In contrast to $Ca_V2.3$wt and Y383 mutants, which experienced clear hyperpolarizing shifts in the presence of exogenous β3, the voltage dependence of inactivation of W386A, W386E, W386Q, W386G, W386F, and W386Y channels was not modulated by β3 (Table 1). The inactivation curves of the W386 mutants fell roughly in three groups. W386E ± β3, W386G ± β3, and W386Q ± β3 inactivated with $E_{0.5,inact} \approx -26$ mV, ~10 mV more positive than the wild-type channel without exogenous β3. W386R ± β3, W386F ± β3, and W386A ± β3 inactivated with $E_{0.5,inact} \approx -36$ mV, which is very similar to the wild-type channel without exogenous β3. Of all the mutants, W386Y ± β3 inactivated at the most negative membrane potentials $E_{0.5,inact} \approx -46$ mV, which is ~10 mV more negative than $Ca_V2.3/\alpha2b\delta$ (no exogenous β3). This result suggests that the higher hydrophilicity of the Tyr residue could influence the voltage-dependent inactivation of $Ca_V2.3$. However, no substitution of W386 could confer the typical β3-induced modulation of kinetics and voltage dependence of inactivation in $Ca_V2.3$.

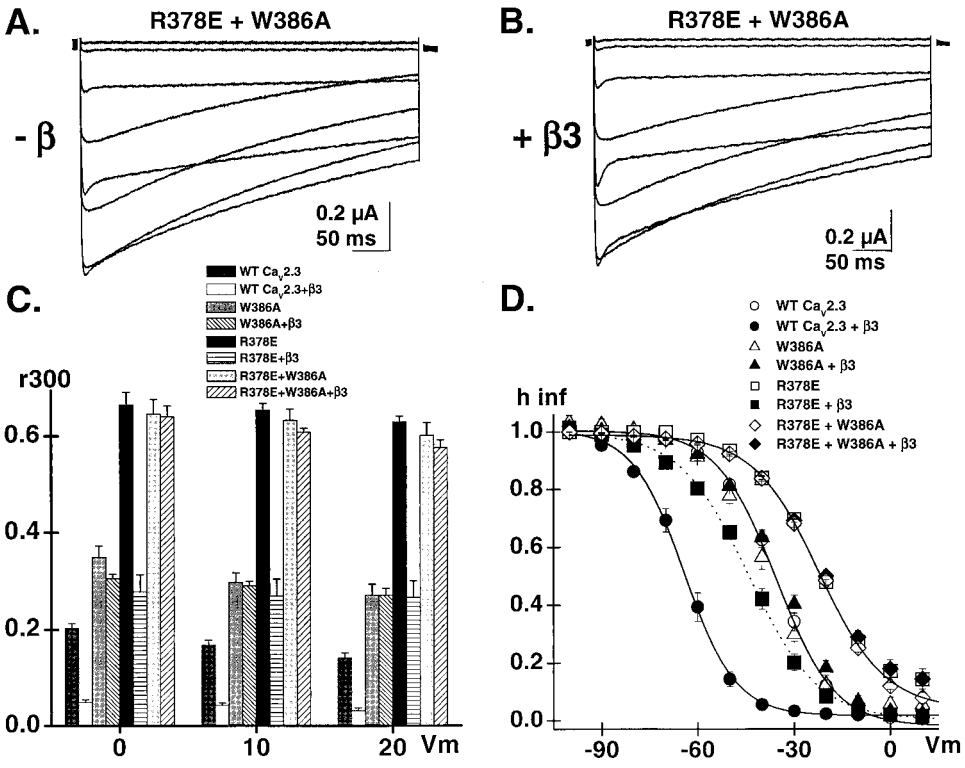

FIGURE 4 Inactivation properties of the double mutant R378E + W386A. (*A* and *B*) Whole-cell current traces were recorded in the presence of 10 mM Ba^{2+} for the double R378E + W386A mutant with α2bδ either without exogenous β3 (*A*) or after co-injection of β3 (*B*). (*C*) The r300 values for the wild-type Ca_V2.3, W386A, R378E, R378E + W386A channels ± β3 (from left to right at each voltage) show that the inactivation kinetics of W386A and R378E + W386A were not significantly accelerated by β3. Whether in the absence or in the presence of β3, the inactivation kinetics of W386A were slower than the wild-type channel but faster than R378E. The R378E + W386A mutant combined the individual properties of R378E and W386A mutants as it inactivated like R378E and did not show any β-subunit-induced modulation. (*D*) The voltage dependence of inactivation was estimated after a series of 5-s conditioning prepulses applied between −100 and +30 mV. The fraction of the non-inactivating current was recorded at the end of the pulse, and data were fitted to the Boltzmann Eq. 1. β3 significantly shifted the voltage dependence to the left for Ca_V2.3wt from −36 ± 3 mV (n = 10) to −64 ± 2 mV (n = 10) and for R378E from −26 ± 2 mV (n = 7) to −44 ± 2 mV (n = 11) but failed to influence the voltage dependence of W386A or W386A + R378E. The complete set of fit values is shown in Table 1.

DISCUSSION

W386 in the AID motif is required for β-subunit binding and modulation of Ca_V2.3

In this study, the molecular determinants of β-subunit binding and modulation in the Ca_V2.3 Ca^{2+} channel were investigated following mutations within the high-affinity β-subunit binding site (AID) of the I-II linker. The AID motif is composed of a stretch of 18 AA located about at the end of IS6 that reads QQxExxLxG*Y*xx*WI*xxxE. Before our study, little was known on the determinants of β-subunit binding and modulation in Ca_V2.3. Landmark studies by the groups of Campbell and deWaard (Pragnell et al., 1994; Witcher et al., 1995; DeWaard et al., 1996; Bichet et al., 2000b) have highlighted the core YWI residues as key determinants of β-subunit binding in Ca_V2.1 (Pragnell et al., 1994; DeWaard et al., 1996). In particular, point mutations of conserved residues QQxExxLxGxxxxxxxxxE did not prevent β1b (Pragnell et al., 1994; DeWaard et al., 1996) or β3 binding (Bichet et al., 2000b) to the I-II linker in Ca_V2.1. We herein confirmed that mutating W386 disrupted β3-subunit overlay binding to AID_E as it was previously shown for AID_A (Bichet et al., 2000b). We further showed that mutations of W386 dramatically decreased the β-subunit modulation of activation and inactivation of Ca_V2.3 channels. In contrast, mutations of the neighboring residue Y383 preserved the β-subunit modulation in the voltage- dependence of activation and inactivation. The strong correlation between β-subunit binding and modulation for W386 hence suggests that W386 constitutes the primary determinant of β-subunit binding and modulation in Ca_V2.3.

One of the novel pieces of information arising from our data turns out to be the strict requirement for a tryptophan at position 386 for β3-subunit binding and modulation. The tryptophan residue at position 386 appears to be an essential structural determinant for β-subunit binding because substitutions with hydrophobic (A, G), hydrophilic (Q, R, E), or

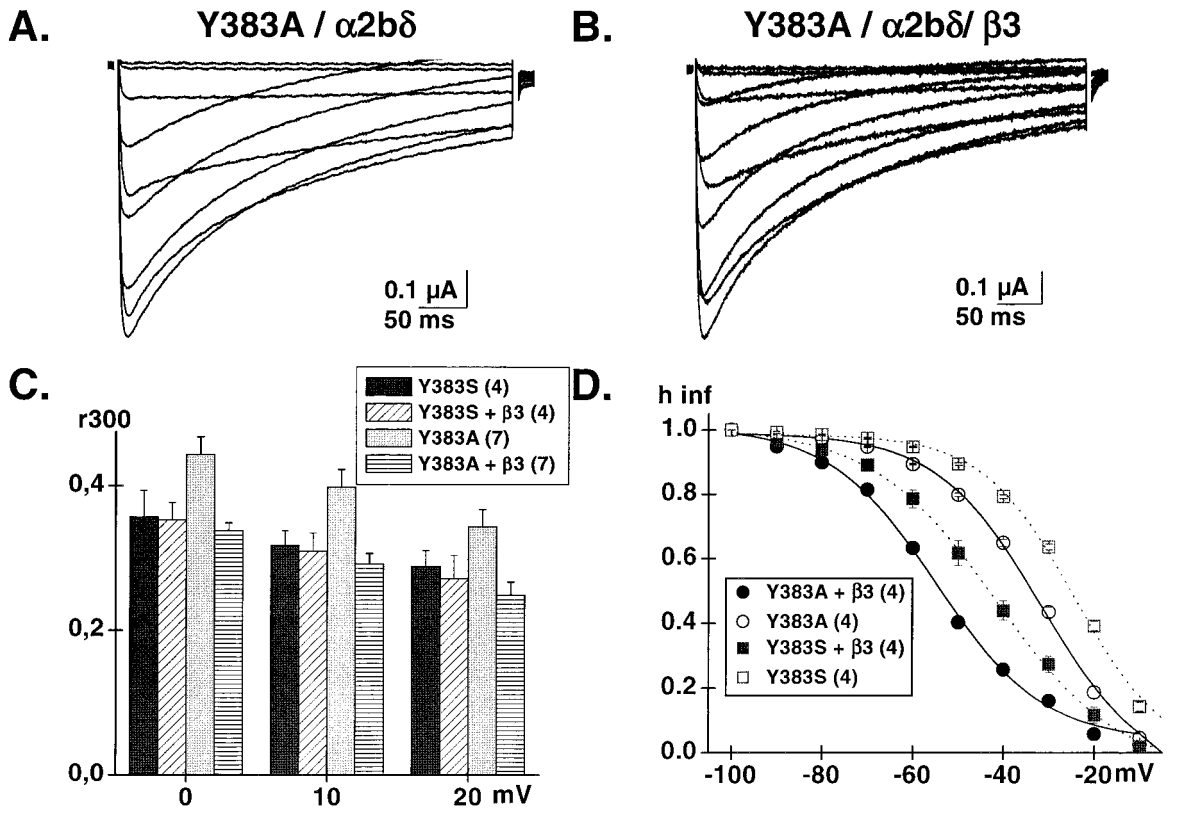

FIGURE 5 Inactivation properties of Y383A and Y383S. (*A* and *B*) Whole-cell current traces were recorded in the presence of 10 mM Ba^{2+} for Y383A mutant with α2bδ without exogenous β3 (*A*) or after co-injection of β3 (*B*). (*C*) The corresponding r300 values are shown for Y383A ± β3 and Y383S ± β3. The inactivation kinetics of Y383S ($n = 4$) was not significantly influenced by β3 ($p > 0.1$), whereas those for Y383A ± β3 ($n = 7$) were significantly different at $p < 0.05$. In the absence or in the presence of β3, the inactivation kinetics of Y383A and Y383S were slower than the wild-type channel and similar to W386A. (*D*) The voltage dependence of inactivation was estimated after a series of 5-s conditioning prepulses applied between −100 and +30 mV. β3 significantly shifted the voltage dependence of inactivation for Y383A from −32 ± 1 mV ($n = 4$) to −55 ± 2 mV ($n = 4$) and for Y383S from −24 ± 1 mV ($n = 4$) to −42 ± 2 mV ($n = 4$). The complete set of values is shown in Table 1.

aromatic (F, Y) residues disrupted β3 binding as well as β-subunit modulation. Previous studies had clearly demonstrated the absence of β1b binding to the WA mutant in $Ca_V2.1$ but reported some level of interaction between β1b and WF/WY mutants (DeWaard et al., 1996), suggesting that the delocalization of π electrons in the phenyl groups could be involved in the interaction with β subunits with $Ca_V2.1$. At this time, we cannot rule out that some level of weak interaction remains between β3 and the W386 mutants. Our experiments were performed with α1:β3 subunits co-injected at a 1:1 molar ratio. Additional experiments aimed at elucidating the affinity of β3 to the AID_E mutants require more sophisticated tools such as fast sampling kinetic analyses (Berteloot et al., 1991; Oulianova et al., 2001) or surface plasmon resonance binding (Canti et al., 2001).

Functional expression of W386 and Y383 mutants in *Xenopus* oocytes

All W386 (A, G, Q, E, R, F, Y) and Y383 (A, S) mutants expressed large inward Ba^{2+} currents. β-Subunits are involved in the membrane trafficking of the α1 subunit in voltage-dependent Ca^{2+} channels where they are actually believed to chaperone the α1 subunit to the membrane (Chien et al., 1995; Neuhuber et al., 1998a; Tareilus et al., 1997; Yamaguchi et al., 1998; Gerster et al., 1999). For instance, the I-II linker was found to regulate the $Ca_V2.1$ channel expression by interacting tightly with a retention signal in the endoplasmic reticulum (ER). The inclusion of the I-II linker of $Ca_V2.1$ inserted at the end of the *Shaker* K^+ channel was shown to prevent the membrane expression of *Shaker* channels (Bichet et al., 2000a). High-affinity binding of β subunits to the AID motif is required to dislodge the I-II linker from the ER, thereby relieving the trafficking clamp and allowing membrane expression of α1 subunits (Bichet et al., 2000a). Unexpectedly, disrupting β-subunit binding to the I-II linker did not eliminate functional channel expression of $Ca_V2.3$ (our results) or $Ca_V2.1$ (Bichet et al., 2000a). Indeed, mutating W386 or Y383 in AID_E as well as deleting 36 AA of AID_A yielded HVA functional channels (Bichet et al., 2000a). It remains to be seen whether mutations of the AID motif lessened the interaction between the I-II

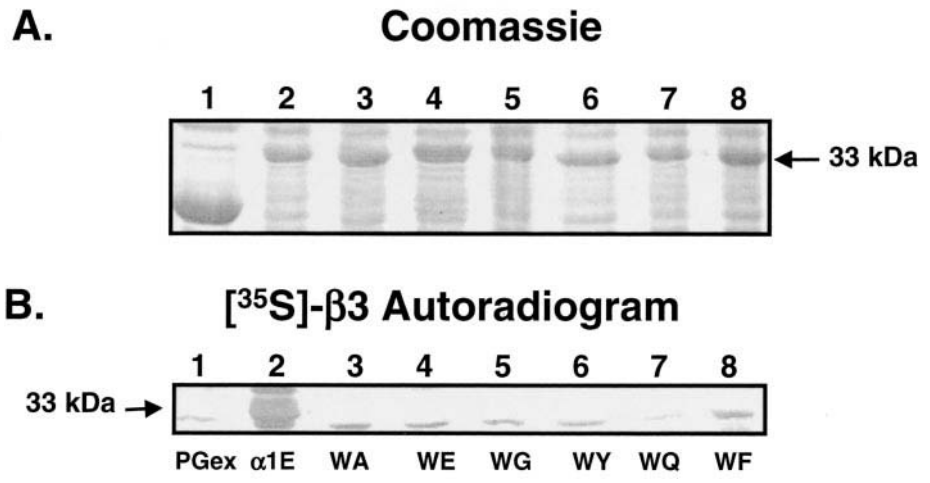

FIGURE 6 β3 does not bind the W386 mutants. (*A*) Coomassie blue-stained SDS-PAGE gel showing the wild-type and the mutant W386 fusion proteins from $Ca_V2.3$. Molecular weight standards are shown to the left. The fusion proteins have a molecular mass of 25 kDa (no insert) or 33 kDa (86AA from the I-II linker). (*B*) Autoradiogram of in vitro translated [^{35}S]methionine β3 overlays on AID_E GST-W386 mutants immobilized on nitrocellulose. The pGex (no insert) is shown as a control (*lane 1*), whereas a strong signal was recorded for the AID motif from the wild-type $Ca_V2.3$ channel (*lane 2*), [^{35}S]β3 binding could not be detected for W386A (*lane 3*), W386E (*lane 4*), W386G (*lane 5*), W386Y (*lane 6*), W386Q (*lane 7*), W386F (*lane 8*).

linker and the retention signal in the ER, thereby decreasing the need for a chaperone auxiliary subunit.

The contribution from additional β-subunit binding sites already identified in other cytoplasmic regions of the α1 subunit in $Ca_V2.1$ and $Ca_V2.3$ using i*n vitro* binding experiments (Birnbaumer et al., 1998; Cens et al., 1998; Olcese et al., 1994; Qin et al., 1997; Walker et al., 1998) remains to be fully investigated in $Ca_V2.3$. Although their functional

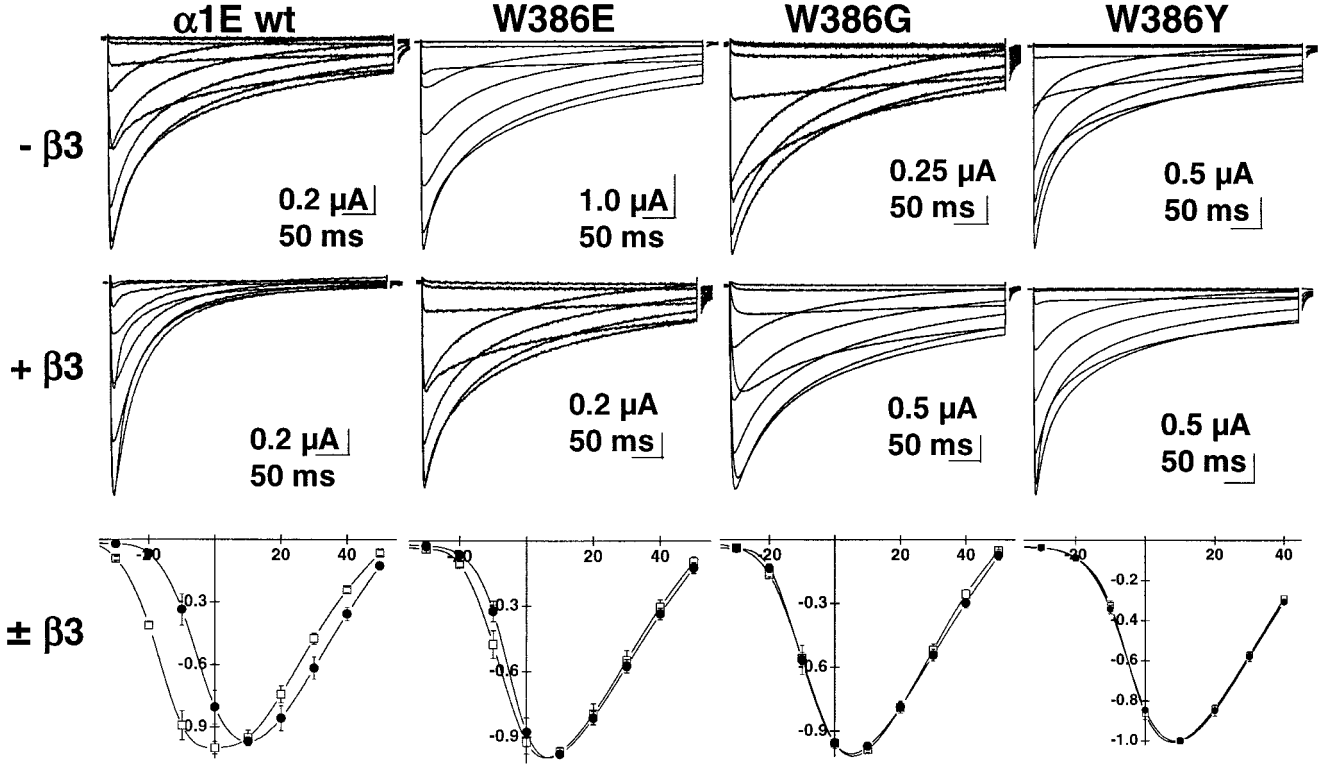

FIGURE 7 W386 mutants are not modulated by β3. Whole-cell currents were recorded in the presence of 10 mM Ba^{2+} for the wild-type $Ca_V2.3$, W386E, W386G, and W386Y with α2bδ in the absence of β3 (*upper panel*) and when coexpressed with β3 (*middle panel*). The inactivation kinetics of the W386 mutants was not accelerated by β3. The peak current voltage relationships were not shifted to the left in the presence of β3 for the W386 mutants as seen on the mean normalized current-voltage relationships (*lower panel*). Identical results were obtained for W386A, W386F, and W386R (not shown).

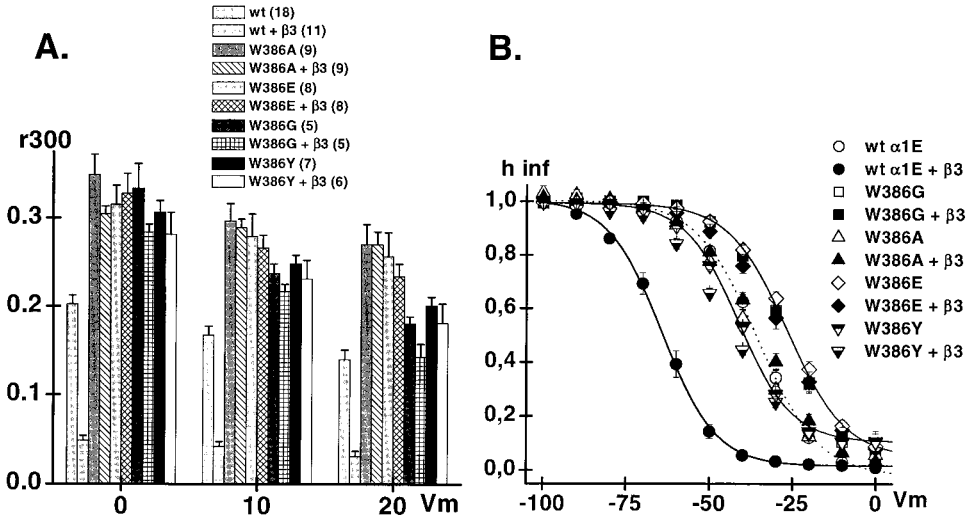

FIGURE 8 Inactivation properties of the W386 mutants (*A*) The cumulative r300 values are shown for the wild-type $Ca_V2.3$, W386A, W386E, W386G, and W386Y ± β3. The inactivation kinetics of W386 mutants was not significantly influenced by β3. Nonetheless, the inactivation kinetics of W386G and W386Y remained voltage dependent and accelerated with depolarization. (*B*) The voltage dependence of inactivation was estimated after a series of 5-s conditioning prepulses applied between −100 and +30 mV. The fraction of the non-inactivating current was recorded at the end of the pulse, and data were fitted to the Boltzmann Eq. 1. β3 had no significant effect on the voltage dependence of inactivation for W386A, W386G, and W386E but barely shifted the $E_{0.5}$ of W386Y to the left ($p > 0.05$). The complete set of fit values is shown in Table 1.

relevance in terms of β-subunit modulation has yet to be established, such binding sites could partially offset the consequences of disrupting the AID motif by providing some level of interaction between α1 and β subunits.

β-Subunit binding is preserved after multiple mutations of nonconserved residues in AID

The molecular determinants of β-subunit binding and functional modulation of $Ca_V2.3$ were investigated following mutations of conserved and nonconserved residues within the high-affinity β-subunit binding site (AID) of the I-II linker. As far as β-subunit binding is concerned, multiple mutations of the nonconserved residues within the AID motif, as in the $Ca_V2.3$ R365G + A366D + I376L + R378E + E379D + N381K + R384L + A385D + D388T + K389Q mutant, did not disrupt [^{35}S]β3 overlay binding to GST fusion proteins from $Ca_V2.3$, suggesting that β3 binding to the I-II linker is not critically sensitive to the nature of residues interwoven in the AID motif. Our findings thus extend previous reports that the equivalent mutation R387E in $Ca_V2.1$ retains the ability to bind [^{35}S]β3 (Bichet et al., 2000b). The binding experiments further agree with our previous report showing that β-subunit modulation of inactivation was preserved in the R378E channel (Berrou et al., 2001). Furthermore, our current study confirmed that the inactivation kinetics of R378E were consistently slower than $Ca_V2.3$wt when expressed under the same subunit background (Figs. 2, 3, 4, 6, and 7). Hence, mutating R378 in $Ca_V2.3$ did not appear to modify significantly the extent to which β subunits regulate inactivation. This contrasts with the recent observation that the similar mutation in $Ca_V2.1$ (R387E) slowed down the inactivation kinetics of $Ca_V2.1$ but only when measured in a β4 background (Geib et al., 2002). Altogether, our data support the conclusion that the changes in the inactivation properties reported for R378E in $Ca_V2.3$ were likely to be conferred by the α1 subunit itself (Berrou et al., 2001).

Role of the I-II linker and β-subunits in the voltage-dependent inactivation of $Ca_V2.3$

Mounting evidence suggests that the I-II linker of HVA α1 subunits behaves as a tethered inactivating blocking particle (Berrou et al., 2001; Stotz and Zamponi, 2001). Besides the control of inactivation, the I-II linker contains, however, other key regulatory sites for channel activity because it anchors β-subunit interaction and provides modulation by G proteins and protein kinase C (DeWaard et al., 1997; Zamponi et al., 1997), which in turn could affect inactivation properties (kinetics and voltage dependence). We attempted to unravel the role of the I-II linker in the functional modulation of $Ca_V2.3$ by investigating the β-subunit binding and modulation as well as the inactivation properties of the R378E, W386, and the R378E + W386A mutants.

The R378E channel displayed decreased inactivation kinetics and voltage dependence, although it preserved typical β3-subunit binding and modulation. Although W386A channels failed to be typically modulated by β3 subunits, their inactivation properties (kinetics and voltage depen-

dence) remained weaker than the wild-type channel expressed under the same conditions. Hence, with the exception of W386G at +20 mV, all W386 mutants inactivated significantly slower than the $Ca_V2.3$wt channel expressed in the absence of β3 subunits. Nonetheless, the voltage dependence of inactivation properties of the W386 mutants appeared to be variable. For instance, although the voltage dependence of inactivation of W386A, W386R, and W386F mutants was indistinguishable from the wild-type $Ca_V2.3/\alpha 2b\delta$ (without β3), the W386E, W386G, and W386Q channels inactivated distinctively at more positive voltages. Furthermore, the tryptophan-to-tyrosine substitution that preserved an aromatic residue at position 386 (W386Y) yielded channels that inactivated at more negative potentials than the wild-type channel expressed without β3 subunits. Interestingly, the slightly less polar phenylalanine residue, albeit bearing a similar phenyl group, behaved like the W386A channel. This observation suggests that mutations of conserved and nonconserved residues alike in the I-II linker could alter the inactivation kinetics of $Ca_V2.3$ channels (Berrou et al., 2001). We examined this proposition by investigating the properties of the double mutant R378E + W386A. The double mutant lacks β3-subunit modulation, but its inactivation properties were shown to be identical to the R378E/$\alpha 2b\delta$ channel. Hence, mutating the neighboring residue W386 does not further decrease the kinetics and voltage dependence of inactivation of R378E. These results suggest altogether that R378 and W386, albeit localized on the same motif, control distinct functions in HVA Ca^{2+} channels and confirm that R378 in the I-II linker is the key determinant of voltage-dependent inactivation in $Ca_V2.3$.

In line with our observations, deWaard and collaborators have recently proposed that the altered inactivation properties of the R387E mutant in $Ca_V2.1$ resulted from the disruption of the intra-subunit interaction between the cytoplasmic I-II and the III-IV linkers (Geib et al., 2002). In their model, the strong interaction between the I-II and the III-IV linkers would prevent fast inactivation kinetics of the wild-type $Ca_V2.1$ channel. The β subunits would then promote faster inactivation kinetics by weakening the linkers' interaction. This stimulating proposition might, however, not extend to all HVA Ca^{2+} channels. In $Ca_V2.1$, R387E was shown to inactivate faster than the wild-type channel in the absence of β4. The situation appears to be different with the R378E mutant in $Ca_V2.3$ as it displayed slower inactivation kinetics and reduced voltage dependence of inactivation as compared with the wild-type channel whether in the presence or absence of coexpressed β3 or β2a subunits (Fig. 2) (Berrou et al., 2001). These contradictory results might either result from intrinsic differences in the inactivation mechanism of HVA Ca^{2+} channels or else reflect β-subunit isoform binding specificity. It has been reported that β4 interacted with relatively high affinity to numerous intracellular loops (Walker et al., 1998, 1999), whereas β1b and β3 displayed a significantly higher affinity for AID in the I-II linker than for any other cytoplasmic loop of $Ca_V2.1$ (Walker et al., 1998, 1999). It hence remains to be seen whether this pattern of selectivity among β subunits is preserved in $Ca_V2.3$ and more specifically in R378E.

We thank Dr. Toni Schneider for the human $Ca_V2.3$ channel, Dr Ed Perez-Reyes for the β_3 and the β2a subunits, Ms Julie Verner for dedicated oocyte culture, Dr. Pierre Bissonnette for discussions, and Dr. Rémy Sauvé for critical reading. L.P. is a senior scholar from the Fonds de la Recherche en Santé du Québec.

This work was supported by the Canadian Heart and Stroke Foundation and by the Canadian Institutes of Health Research grant MOP13390 to L.P.

REFERENCES

Beguin, P., K. Nagashima, T. Gonoi, T. Shibasaki, K. Takahashi, Y. Kashima, N. Ozaki, K. Geering, T. Iwanaga, and S. Seino. 2001. Regulation of Ca^{2+} channel expression at the cell surface by the small G-protein kir/Gem. *Nature.* 411:701–706.

Bell, D. C., A. J. Butcher, N. S. Berrow, K. M. Page, P. F. Brust, A. Nesterova, K. A. Stauderman, G. R. Seabrook, B. Nurnberg, and A. C. Dolphin. 2001. Biophysical properties, pharmacology, and modulation of human, neuronal L-type (α(1D), $Ca_V1.3$) voltage-dependent calcium currents. *J. Neurophysiol.* 85:816–827.

Bernatchez, G., L. Berrou, Z. Benakezouh, J. Ducay, and L. Parent. 2001a. Role of repeat I in the fast inactivation kinetics of the $Ca_V2.3$ channel. *Biochim. Biophys. Acta* 1514:217–229.

Bernatchez, G., R. Sauvé, and L. Parent. 2001b. State-dependent inhibition of inactivation-deficient $Ca_V1.2$ and $Ca_V2.3$ channels by mibefradil. *J. Membr. Biol.* 184:143–159.

Bernatchez, G., D. Talwar, and L. Parent. 1998. Mutations in the EF-hand motif of the cardiac α_{1C} calcium channel impair the inactivation of barium currents. *Biophys. J.* 75:1727–1739.

Berrou, L., G. Bernatchez, and L. Parent. 2001. Molecular determinants of inactivation within the I-II linker of α1E ($Ca_V2.3$) Ca^{2+} channels. *Biophys. J.* 80:215–228.

Berteloot, A., C. Malo, S. Breton, and M. Brunette. 1991. Fast sampling, rapid filtration apparatus: principal characteristics and validation from studies of D-glucose transport in human jejunal brush-border membrane vesicles. *J. Membr. Biol.* 122:111–125.

Bichet, D., V. Cornet, S. Geib, E. Carlier, S. Volsen, T. Hoshi, Y. Mori, and M. DeWaard. 2000a. The I-II loop of the Ca^{2+} channel α1 subunit contains an endoplasmic reticulum retention signal antagonized by the β subunit. *Neuron.* 25:177–190.

Bichet, D., C. Lecomte, J. M. Sabatier, R. Felix, and M. DeWaard. 2000b. Reversibility of the Ca^{2+} channel α1-β subunit interaction. *Biochem. Biophys. Res. Commun.* 277:729–735.

Biel, M., R. Hullin, S. Freundner, D. Singer, N. Dascal, V. Flockerzi, and F. Hofmann. 1991. Tissue-specific expression of high-voltage-activated dihydropyridine-sensitive L-type calcium channels. *Eur. J. Biochem.* 200:81–88.

Birnbaumer, L., N. Qin, R. Olcese, E. Tareilus, D. Platano, J. Costantin, and E. Stefani. 1998. Structures and functions of calcium channel beta subunits. *J. Bioenerg. Biomembr.* 30:357–375.

Brice, N. L., N. S. Berrow, V. Campbell, K. M. Page, K. Brickley, I. Tedder, and A. C. Dolphin. 1997. Importance of the different β subunits in the membrane expression of the α1A and α2 calcium channel subunits: studies using a depolarization-sensitive α1A antibody. *Eur. J. Neurosci.* 9:749–759.

Canti, C., A. Davies, N. S. Berrow, A. J. Butcher, K. M. Page, and A. C. Dolphin. 2001. Evidence for two concentration-dependent processes for β-subunit effects on α1B calcium channels. *Biophys. J.* 81:1439–1451.

Castellano, A., X. Wei, L. Birnbaumer, and E. Perez-Reyes. 1993. Cloning and expression of a third calcium channel β subunit. *J. Biol. Chem.* 268:3450–3455.

Catterall, W. A. 1991. Functional subunit structure of voltage-gated calcium channels. *Science.* 250:1499–1500.

Cens, T., S. Restituito, S. Galas, and P. Charnet. 1999. Voltage and calcium use the same molecular determinants to inactivate calcium channels. *J. Biol. Chem.* 274:5483–5490.

Cens, T., S. Restituito, A. Vallentin, and P. Charnet. 1998. Promotion and inhibition of L-type Ca^{2+} channel facilitation by distinct domains of the subunit. *J. Biol. Chem.* 273:18308–18315.

Chien, A. J., K. M. Carr, R. E. Shirokov, E. Rios, and M. M. Hosey. 1996. Identification of palmitoylation sites within the L-type calcium channel β2a subunit and effects on channel function. *J. Biol. Chem.* 271: 26465–26468.

Chien, A. J. and M. M. Hosey. 1998. Post-translational modifications of β subunits of voltage-dependent calcium channels. *J. Bioenerg. Biomembr.* 30:377–386.

Chien, A. J., X. Zhao, R. E. Shirokov, T. S. Puri, C. F. Chang, D. Sun, E. Rios, and M. M. Hosey. 1995. Roles of a membrane-localized β subunit in the formation and targeting of functional L-type Ca^{2+} channels. *J. Biol. Chem.* 270:30036–30044.

DeWaard, M., and K. P. Campbell. 1995. Subunit regulation of the neuronal α_{1A} Ca^{2+} channel expressed in *Xenopus* oocytes. *J. Physiol. (Lond.).* 485:619–634.

DeWaard, M., H. Liu, D. Walker, V. E. Scott, C. A. Gurnett, and K. P. Campbell. 1997. Direct binding of G-protein βγ complex to voltage-dependent calcium channels. *Nature.* 385:446–500.

DeWaard, M., V. E. Scott, M. Pragnell, and K. P. Campbell. 1996. Identification of critical amino acids involved in α_1-β interaction in voltage-dependent Ca^{2+} channels. *FEBS Lett.* 380:272–276.

DeWaard, M., D. R. Witcher, M. Pragnell, H. Liu, and K. P. Campbell. 1995. Properties of the α_1-β anchoring site in voltage-dependent Ca^{2+} channels. *J. Biol. Chem.* 270:12056–12064.

Gasparini, S., A. M. Kasyanov, D. Pietrobon, L. L. Voronin, and E. Cherubini. 2001. Presynaptic R-type calcium channels contribute to fast excitatory synaptic transmission in the rat hippocampus. *J. Neurosci.* 21:8715–8721.

Geib, S., G. Sandoz, V. Cornet, K. Mabrouk, O. Fund-Saunier, D. Bichet, M. Villaz, T. Hoshi, J. M. Sabatier, and M. DeWaard. 2002. The interaction between the I-II loop and the III-IV loop of Cav 2.1 contributes to voltage-dependent inactivation in a β-dependent manner. *J. Biol. Chem.* 277:10003–10013.

Gerster, U., B. Neuhuber, K. Groschner, J. Striessnig, and B. E. Flucher. 1999. Current modulation and membrane targeting of the calcium channel α1C subunit are independent functions of the β subunit. *J. Physiol. (Lond.).* 517:353–368.

Herlitze, S., G. H. Hockerman, T. Scheuer, and W. A. Catterall. 1997. Molecular determinants of inactivation and G protein modulation in the intracellular loop connecting domains I and II of the calcium channel α_{1A} subunit. *Proc. Natl. Acad. Sci. U.S.A.* 94:1512–1516.

Jean, K., G. Bernatchez, L. Garneau, H. Klein, R. Sauvé, and L. Parent. 2002. The role of Asp residues in Ca affinity and permeation in the distal ECaC1 channel. *Am. J. Physiol. Cell Physiol.* 282:C665–C672.

Jones, L. P., S. K. Wei, and D. T. Yue. 1998. Mechanism of auxiliary subunit modulation of neuronal α1E calcium channels. *J. Gen. Physiol.* 112:125–143.

Kim, D., I. Song, S. Keum, T. Lee, M. Jeong, S. Kim, M. W. McEnery, and H. Shin. 2001. Lack of the burst firing of thalamocortical relay neurons and resistance to absence seizures in mice lacking α1G T-type Ca^{2+} channels. *Neuron.* 31:35–45.

Mangoni, M. E., T. Cens, C. Dalle, J. Nargeot, and P. Charnet. 1997. Characterisation of α1A Ba^{2+}, Sr^{2+} and Ca^{2+} currents recorded with the ancillary β 1–4 subunits. *Receptors Channels.* 5:1–14.

Neuhuber, B., U. Gerster, F. Doring, H. Glossmann, T. Tanabe, and B. E. Flucher. 1998a. Association of calcium channel α1S and β1a subunits is required for the targeting of β1a but not of α1S into skeletal muscle triads. *Proc. Natl. Acad. Sci. U.S.A.* 95:5015–5020.

Neuhuber, B., U. Gerster, J. Mitterdorfer, H. Glossmann, and B. E. Flucher. 1998b. Differential effects of Ca^{2+} channel β1a and β2a subunits on complex formation with α1S and on current expression in tsA201 cells. *J. Biol. Chem.* 273:9110–9118.

Olcese, R., N. Qin, T. Schneider, A. Neely, X. Wei, E. Stefani, and L. Birnbaumer. 1994. The amino terminus of a calcium channel beta subunit sets rates of channel inactivation independently of the subunit's effect on activation. *Neuron.* 13:1433–1438.

Oulianova, N., S. Falk, and A. Berteloot. 2001. Two-step mechanism of phlorizin binding to the SGLT1 protein in the kidney. *J. Membr. Biol.* 179:223–242.

Page, K. M., G. J. Stephens, N. S. Berrow, and A. C. Dolphin. 1997. The intracellular loop between domains I and II of the B-type calcium channel confers aspects of G-protein sensitivity to the E-type calcium channel. *J. Neurosci.* 17:1330–1338.

Parent, L., M. Gopalakrishnan, A. E. Lacerda, X. Wei, and E. Perez-Reyes. 1995. Voltage-dependent inactivation in a cardiac-skeletal chimeric calcium channel. *FEBS Lett.* 360:144–150.

Parent, L., T. Schneider, C. P. Moore, and D. Talwar. 1997. Subunit regulation of the humain brain α_{1E} calcium channel. *J. Membr. Biol.* 160:127–140.

Perez-Reyes, E., A. Castellano, H. S. Kim, P. Bertrand, E. Baggstrom, A. E. Lacerda, X. Y. Wei, and L. Birnbaumer. 1992. Cloning and expression of a cardiac/brain β subunit of the L-type calcium channel. *J. Biol. Chem.* 267:1792–1797.

Piedras-Renteria, E. S. and R. W. Tsien. 1998. Antisense oligonucleotides against α_{1E} reduce R-type calcium currents in calcium currents in cerebellar granule cells. *Proc. Natl. Acad. Sci. U.S.A.* 95:7760–7765.

Pragnell, M., M. DeWaard, Y. Mori, T. Tanabe, T. P. Snutch, and K. P. Campbell. 1994. Calcium channel β-subunit binds to a conserved motif in the I-II cytoplasmic linker of the α_1-subunit. *Nature.* 368:67–70.

Qin, N., D. Platano, R. Olcese, J. L. Costantin, E. Stefani, and L. Birnbaumer. 1998. Unique regulatory properties of the type 2a Ca^{2+} channel β subunit caused by palmitoylation. *Proc. Natl. Acad. Sci. U.S.A.* 95: 4690–4695.

Qin, N., D. Platano, R. Olcese, E. Stefani, and L. Birnbaumer. 1997. Direct interaction of $G_{\beta\gamma}$ with a C-terminal $G_{\beta\gamma}$ binding domain of the Ca^{2+} channel α_1 subunit is responsible for channel inhibition by G protein-coupled receptors. *Proc. Natl. Acad. Sci. U.S.A.* 94:8866–8871.

Randall, A. D. and R. W. Tsien. 1997. Contrasting biophysical and pharmacological properties of T-type and R-type calcium channels. *Neuropharmacology.* 36:879–893.

Restituito, S., T. Cens, C. Barrere, S. Geib, S. Galas, W. M. De, and P. Charnet. 2000. The β2a subunit is a molecular groom for the Ca^{2+} channel inactivation gate. *J. Neurosci.* 20:9046–9052.

Saegusa, H., T. Kurihara, S. Zong, O. Minowa, A. Kazuno, W. Han, Y. Matsuda, H. Yamanaka, M. Osanai, T. Noda, and T. Tanabe. 2000. Altered pain responses in mice lacking α1E subunit of the voltage-dependent Ca^{2+} channel. *Proc. Natl. Acad. Sci. U.S.A.* 97:6132–6137.

Sambrook, J., E. F. Fritsch, and T. Maniatis. 1989. Molecular Cloning: A Laboratory Manual, 2nd ed. Cold Spring Harbor Laboratory Press, Cold Spring Harbor, NY.

Schneider, T., X. Wei, R. Olcese, J. L. Costantin, A. Neely, P. Palade, E. Perez-Reyes, N. Qin, J. Zhou, G. D. Crawford, Smith, R. G., Appel, S. H., Stefani, E., and Birnbaumer L. 1994. Molecular analysis and functional expression of the human type E neuronal Ca^{2+} channel α_1 subunit. *Receptors Channels.* 2:255–270.

Soong, T. W., A. Stea, C. D. Hodson, S. J. Dubel, S. R. Vincent, and T. P. Snutch. 1993. Structure and functional expression of a member of the low voltage-activated calcium channel family. *Science.* 260:1133–1136.

Stea, A., W. J. Tomlinson, T. W. Soong, E. Bourinet, S. J. Dubel, S. R. Vincent, and T. P. Snutch. 1994. Localization and functional properties of a rat brain α 1A calcium channel reflect similarities to neuronal Q- and P-type channels. *Proc. Natl. Acad. Sci. U.S.A.* 91:10576–10580.

Stephens, G. J., K. M. Page, Y. Bogdanov, and A. C. Dolphin. 2000. The α1B Ca^{2+} channel amino terminus contributes determinants for subunit-mediated voltage-dependent inactivation properties. *J. Physiol. (Lond.).* 525:377–390.

Stotz, S. C. and G. W. Zamponi. 2001. Structural determinants of fast inactivation of high voltage-activated Ca^{2+} channels. *Trends Neurosci.* 24:176–181.

Tareilus, E., M. Roux, N. Qin, R. Olcese, J. Zhou, E. Stefani, and L. Birnbaumer. 1997. A *Xenopus* oocyte β subunit: evidence for a role in

the assembly/expression of voltage-gated calcium channels that is separate from its role as a regulatory subunit. *Proc. Natl. Acad. Sci. U.S.A.* 94:1703–1708.

Vajna, R., U. Klockner, A. Pereverzev, M. Weiergraber, X. Chen, G. Miljanich, N. Klugbauer, J. Hescheler, E. Perez-Reyes, and T. Schneider. 2001. Functional coupling between 'R-type' Ca^{2+} channels and insulin secretion in the insulinoma cell line INS-1. *Eur. J. Biochem.* 268:1066–1075.

Walker, D., D. Bichet, K. P. Campbell, and M. DeWaard. 1998. A β_4 isoform-specific interaction site in the carboxyl-terminal region of the voltage-dependent Ca^{2+} channel α_{1A} subunit. *J. Biol. Chem.* 273: 2361–2367.

Walker, D., D. Bichet, S. Geib, E. Mori, V. Cornet, T. P. Snutch, Y. Mori, and M. DeWaard. 1999. A new β subtype-specific interaction in α1A subunit controls P/Q-type Ca^{2+} channel activation. *J. Biol. Chem.* 274: 12383–12390.

Walker, D., and M. DeWaard. 1998. Subunit interaction sites in voltage-dependent Ca^{2+} channels: role in channel function. *Trends Neurosci.* 21:148–154.

Wang, G., G. Dayanithi, R. Newcomb, and J. R. Lemos. 1999. An R-type Ca^{2+} current in neurohypophysial terminals preferentially regulates oxytocin secretion. *J. Neurosci.* 19:9235–9241.

Williams, M. E., D. H. Feldman, A. F. McCue, R. Brenner, G. Velicelebi, S. B. Ellis, and M. M. Harpold. 1992. Structure and functional expression of α_1, α_2, and β subunits of a novel human neuronal calcium channel subtype. *Neuron.* 8:71–84.

Witcher, D. R., W. M. De, H. Liu, M. Pragnell, and K. P. Campbell. 1995. Association of native Ca^{2+} channel beta subunits with the α_1 subunit interaction domain. *J. Biol. Chem.* 270:18088–18093.

Yamaguchi, H., M. Hara, M. Strobeck, K. Fukasawa, A. Schwartz, and G. Varadi. 1998. Multiple modulation pathways of calcium channel activity by a β subunit: direct evidence of β subunit participation in membrane trafficking of the α1C subunit. *J. Biol. Chem.* 273: 19348–19356.

Zamponi, G. W., E. Bourinet, D. Nelson, J. Nargeot, and T. P. Snutch. 1997. Crosstalk between G proteins and protein kinase C mediated by the calcium channel α1 subunit. *Nature.* 385:442–446.